Stress tensor computation from earthquake fault-plane solutions: an application to seismic swarms at Mt. Etna volcano (Italy)

Stefano Gresta and Carla Musumeci
Istituto di Geologia e Geofisica, Università di Catania, Italy

Abstract
Fault-plane solutions of some tens of local earthquakes which occurred at Mt. Etna volcano during 1983-1986 have been inverted for stress tensor parameters by the algorithm of Gephart and Forsyth (1984). Three seismic sequences were focused on which respectively occurred during a flank eruption (June 1983), just after the end of a subterminal eruption (October 1984) and during an inter-eruptive period (May 1986). The application to the three sets of data of both the «approximate» and the «exact» methods evidenced the stability of results, and the stress directions are well defined in spite of the small number of events used for the inversion. The σ_1 obtained agrees with the regional tectonic framework, nearly horizontal and oriented N-S, only in the shallow crust, and just after the 1984 eruption. This supports the hypothesis of a tectonic control on the end of the eruptive activities at Mt. Etna. Conversely, results concerning the depth range 10-30 km are in apparent disagreement with other investigations (Cocina *et al.*, 1997), as well as with the regional tectonics. The stress was here found homogeneous, but with σ_1 respectively trending ENE-WSW (June 1983) and E-W (May 1986). We suggest that the stress field could be temporarily modified by a local stress regime driven by the intrusion of uprising magma.

Key words *Mt. Etna – fault-plane solutions – inversion – stress field*

1. Introduction

Mount Etna is a composite strato-volcano located on the eastern margin of Sicily with a basal diameter of about 40 km, and a height of about 3350 m. The volcanic edifice results from a succession of quiet lava eruptions and intense explosive episodes associated with caldera collapses, while its present activity can be roughly divided into persistent activity at summit craters and flank eruptions (Cristofolini *et al.*, 1988).

The volcano lies in a geodynamically complex region dominated by the Africa-Europe N-S slow convergence and by tensional processes at the Ionian boundary of Sicily and in the Calabrian arc (Ghisetti, 1984; Ben Avraham *et al.*, 1990).

The eastern flank of Mt. Etna shows a high degree of tectonization (with a large number of faults), and it is the volcano sector where the greatest amount of lava emission has taken place. Most of the shallowest seismicity (focal depth less than 5 km) occurs in this sector, wheareas deeper events (up to about 30 km) are more frequent on the western side (Gresta *et al.*, 1990). Earthquakes occurring in the

Mailing address: Dr. Carla Musumeci, Istituto di Geologia e Geofisica, Università di Catania, Corso Italia 55, 95129 Catania, Italy; e-mail: musumeci@mbox.unict.it

Etnean area are characterized by magnitudes usually less than 4.0, and have a tectonic origin, involving the brittle basement of the volcano (Patanè D. *et al.*, 1994).

Looking at previous studies on the stress field acting on Mt. Etna, *in situ* stress measurements and geostructural investigations suggested that a compression *ca.* N-S trending was acting until the middle Pleistocene on the whole area; wheareas it should be confined to the solely northernmost part of Etna, while an extensional stress field extends from this area southward to the Hyblean region (Bousquet *et al.*, 1987).

Short-term time variations of the b coefficient at the frequency-magnitude relationship were first observed at Etna, some weeks before the start of the two flank eruptions of 1981 and 1983 (Gresta and Patanè, 1983a,b). They have been interpreted as small but rapid changes in the stress field acting on the upper parts of the volcano. Magma injection was invoked for these extremely local stress variations (Gresta and Patanè, 1983b), even if it was evident that regional tectonics play an important role in determining both seismic and volcanic phenomena at Mt. Etna (Gresta and Patanè, 1987). Further investigations on the time evolution of the b coefficient and of seismic attenuation Q_c during 1981-1987 evidenced significant changes of both parameters, suggesting long-period variations of the physical state of the volcano (Patanè *et al.*, 1992).

Pioneer studies (Scarpa *et al.*, 1983; Gresta *et al.*, 1985) using Fault-Plane Solutions (hereafter FPS) suggested that normal faulting is dominant in the shallow crust ($h < 7$ km), whereas normal and thrust faulting coexist for deeper events. This difference was attributed (Scarpa *et al.*, 1983) to the superposition of an extensional regime on an older, partially relaxed, deeper compressional one.

More recently, tectonic forces have been invoked as causing the end of a long eruption, by means of a «locking mechanism», while the increase in magma pressure at depth might be responsible for local re-orientation of the stress field (Patanè G. *et al.*, 1994). This latter hypothesis was also supported by Bonaccorso *et al.* (1996), who suggested a local inversion of the stress field acting on the upper crust ($h < 10$ km), starting around two months before the onset of the 1991-1993 eruption, and disappearing at its end.

Finally, results from stress inversion (Cocina *et al.*, 1997) allowed a homogeneous stress on the western side of the volcano, at depths between 10 and 30 km, characterized by a low-dip N-S trending σ_1, in agreement with the regional compressive tectonics. Some stress heterogeneity was here found at shallower depths. Conversely, the stress appeared more complex on the eastern side, where no uniform stress models have been able to explain the available FPSs.

The goal of the present work was to relocate earthquakes which occurred at Mt. Etna volcano during 1983-1986, to obtain focal mechanisms of selected swarms, and to use FPSs as input data for stress tensor inversion by the algorithm of Gephart and Forsyth (1984).

2. The method

Several inverse techniques have been devised to find the stress field most consistent with a heterogeneous set of focal mechanism data (*e.g.*, Angelier, 1979, 1984; Gephart and Forsyth, 1984; Michael, 1984, 1987; Gephart, 1990; Rivera and Cisternas, 1990). Such techniques are capable of solving four of the six independent components of the stress tensor, commonly parametrized by three unit vectors which specify the maximum (σ_1), minimum (σ_3), and intermediate (σ_2) compressive principal-stress axis orientations, and by a scalar which describes the relative magnitudes of the principal stresses and hence constrains the shape of the stress ellipsoid: $R = (\sigma_2 - \sigma_1)/(\sigma_3 - \sigma_1)$. When σ_2 and σ_3 are nearly equivalent (uniaxial deviatoric compression), R approaches 1, and when σ_2 and σ_1 are nearly equivalent (biaxial deviatoric compression), R approaches 0. The two remaining stress tensor parameters (characterizing the absolute magnitude of the deviatoric and isotropic stresses) cannot be determined from focal mechanism data.

To estimate the principal-stress orientations and relative magnitudes, we used Gephart's (1990) Focal Mechanism Stress Inversion program (FMSI) which implemented the previous algorithm of Gephart and Forsyth (1984). This method identifies stress models that are most consistent with a given set of focal mechanisms by a solution space search. It works under the following basic assumptions: i) stress is uniform in the rock volume related to the seismic sample under investigation; ii) earthquakes are due to shear dislocations along pre-existing faults; iii) slip occurs in the direction of the resolved shear stress on the fault plane.

In order to define discrepancies between the stress tensor and observations (FPS), a misfit variable is introduced; the misfit of a single focal mechanism is defined as the minimum rotation about any arbitrary axis that brings one of the nodal planes, together with its slip direction and sense of slip, into an orientation that is consistent with the stress model. The minimum average misfit, indicated by F, is made up of two components: the contribution from errors in the fault plane solutions, and the heterogeneity in the stress field that causes the earthquakes in the data set. We have assumed that the condition of the homogeneous stress tensor is fulfilled if values of F are smaller than 4°, and that it is not fulfilled if $F > 6°$. In the range $4° < F < 6°$, the solution is considered to be acceptable, but may reflect some heterogeneity. When stress is not homogeneous for a given data set, other attempts are made by inverting sub-sets corresponding to time sub-intervals and/or space sub-volumes.

In implementing the grid search, σ_1 is firstly fixed, and a misfit measure is calculated for a range of R and for consistent values of σ_2 and σ_3. The process is progressively repeated using new trial values of σ_1, which are selected from a regular grid superimposed on an equal-area projection.

The limit of the 90% confidence regions of the orientation of the principal stress axes is the second criterion for judging the quality of the inversion results. Using standard statistical methods for one-norm misfits (Parker and McNutt, 1980) we construct confidence limits for the models in a four-parameter space. A stress tensor is accepted if the 90% confidence regions of the greatest and the least principal components of the tensor are well constrained. In this way we are able to realistically assess the uncertainty in the analysis.

For the stress inversion of focal mechanism data we used two of the three algorithms allowed by FMSI: i) the «exact» method, which requires lengthy computations to determine the precise rotation about any axis of general orientations; ii) the «approximate» method, which involves much less computation but finds only a rough approximation of the minimum rotation needed about one of the three axes of the fault plane geometry.

For this reason we can perform initial wide-ranging grid searches using the approximate method; then the results of that analysis define the range over which the exact method is applied. In so doing, we reduce the time cost of the whole procedure.

Since the approximate method finds only a rough approximation of the minimum rotation needed to match an observed fault plane with one consistent with a given stress model, we can also use the exact method with a variance about the central primary stress axis to determine the precise rotation about any axis of general orientations. In order to define the stress tensor we may compare the different applications.

Our goal will be to find the set of stresses most nearly consistent with all the observed focal mechanisms.

3. The data

The 1983-1986 time interval was considered because a temporary seismic network was installed at Mt. Etna by IRIGM of Grenoble, to complete the permanent one by University of Catania (*i.e.*, Glot *et al.*, 1984). Up to 18 stations were working during the period of investigation, and fig. 1 shows the configuration of both seismic networks.

More than 2400 local shocks were recorded in at least four stations, during the considered period. Hypocentral locations of the events were carried out using the HYPO71 program

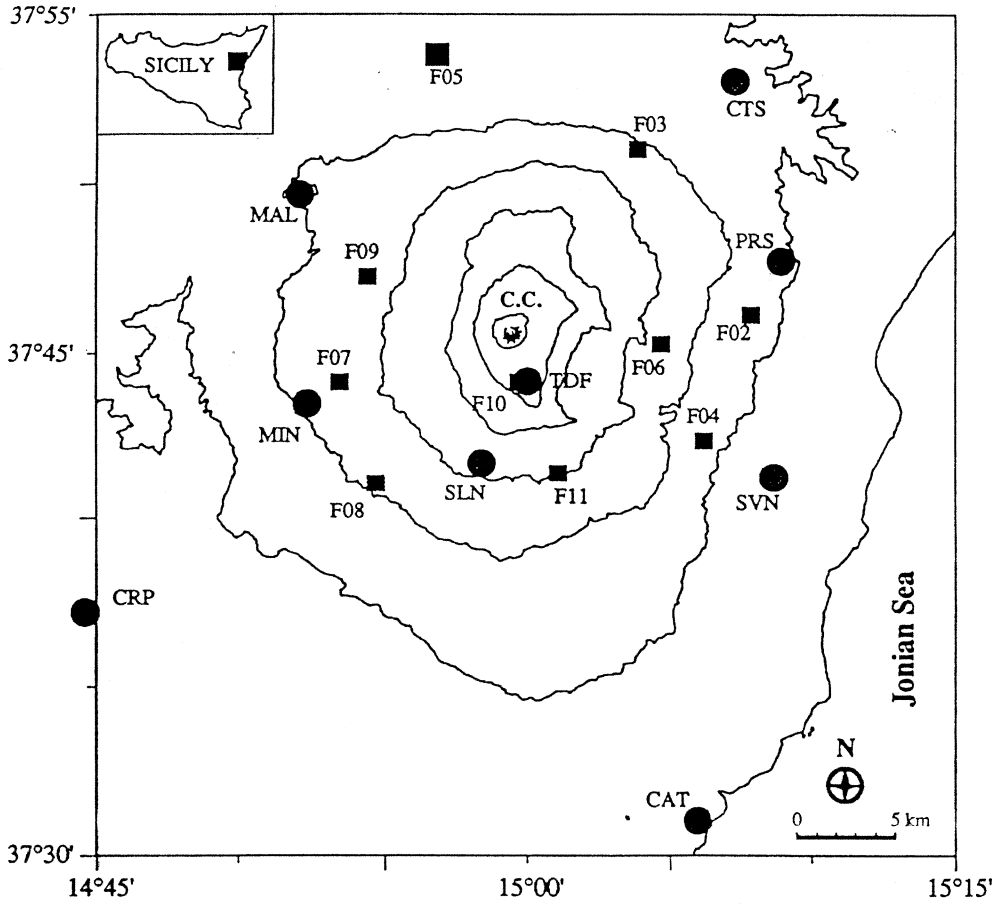

Fig. 1. Sketch map of seismic networks (Catania University = dots, Grenoble IRIGM = squares) at Mt. Etna during 1983-1986; C.C. = Central Craters.

(Lee and Lahr, 1975), and the velocity model proposed for the Etnean region by Hirn *et al.* (1991). The hypocentral depths range from 0 to 30 km. Because the general low magnitudes of the events and the often high noise level, most of the locations are very poor (quality D, see table I).

In order to obtain focal mechanisms we have retained only the earthquakes with: i) A, B, C quality; ii) number of *P*-polarities greater than 7; iii) epicentral and focal depth errors less than 3 and 5 km, respectively. The data set was dramatically reduced, and for the whole considered period only about 370 events were obtained (see table I).

FPS were computed by the FPFIT code (Reasenberg and Oppenheimer, 1985) and only one hundred of reliable focal mechanisms resulted.

The space-time clustering features of the seismic activity which occurred at Etna volcano during 1983-1987 were statistically analyzed by Gasperini *et al.* (1992); their conclusions were: 1) clustering mainly originates from swarm-type sequences; 2) the largest events ($M \geq 3.5$) appear unclustered; 3) no co-

herent spatial migration of the clusters has been found; 4) sequences identified using threshold magnitudes of both 2.5 and 3.0 appear independent in both space and time to eruptions.

We considered FPS for three of the sequences reported in table II, because they are representative of three different stages of the volcano.

The first swarm considered occurred on the western flank of Etna, during the March-August 1983 flank eruption. It is a clear example (see Gresta and Patanè, 1987) of deep (10-25 km) earthquakes occurring when an eruption is still ongoing.

The second seismic sequence represents an unusual behaviour of the volcano. This intense shallow swarm (more than 1000 earthquakes

Table I. Statistical parameters for the hypocentral locations of earthquakes which occurred at Mt. Etna during 1983-1986. The first column reports data for the whole located events, while the second one only for events selected in order to compute FPSs.

Year	Complete data set	NO ≥ 8; GAP ≤ 200°; RMS ≤ 0.8 ERH ≤ 3 km; ERZ ≤ 5 km
1983	No. 495	No. 33
	A = 0 (0%)	A = 0 (0%)
	B = 9 (1.8%)	B = 8 (24.2%)
	C = 95 (19.2%)	C = 20 (60.6%)
	D = 391 (79.0%)	D = 5 (15.2%)
1984	No. 646	No. 177
	A = 1 (0.2%)	A = 1 (0.6%)
	B = 60 (9.3%)	B = 49 (27.7%)
	C = 294 (45.5%)	C = 117 (66.1%)
	D = 291 (45.0%)	D = 10 (5.6%)
1985	No. 571	No. 106
	A = 0 (0.0%)	A = 0 (0%)
	B = 36 (6.3%)	B = 27 (25.0%)
	C = 229 (40.1%)	C = 62 (58.5%)
	D = 306 (53.6%)	D = 17 (16.0%)
1986	No. 694	No. 104
	A = 0 (0%)	A = 0 (0%)
	B = 20 (2.9%)	B = 11 (10.6%)
	C = 223 (32.1%)	C = 79 (76.0%)
	D = 451 (65.0%)	D = 14 (13.5%)
1983-1986	No. 2406	No. 420

Table II. List of the eruptions and of the most important seismic sequences ($M > 2.2$) at Mt. Etna volcano during 1983-1986. Start, end, number of earthquakes and lava output are respectively reported (in bold data relating to the three seismic swarms here studied).

Seismic sequences			Eruptions		
Start	End	Number of events	Start	End	Lava volumes (10^6 m^3)
1983 06 03	**1983 06 04**	**22**	1983 03 28	1983 08 06	75
1983 08 30	1983 11 01	117			
1983 11 11	1983 12 16	37			
1984 05 31	1984 07 07	26	1984 04 27	1984 10 16	10
1984 07 19	1984 09 02	55			
1984 10 16	**1985 01 07**	**271**			
1985 01 20	1985 03 25	53	1985 03 10	1985 07 13	30
1985 11 19	1986 02 11	154	1985 12 25	1985 12 31	1
1986 02 20	1986 03 21	28			
1986 05 07	**1986 05 20**	**122**			
1986 09 30	1986 10 23	40	1986 09 13	1986 09 24	1
1986 10 29	1986 11 05	26	1986 10 30	1987 02 28	60

with $M > 2.0$ during two weeks) started just at the end of a long (April 27-October 16, 1984) subterminal eruption. The seismic activity involved almost the whole eastern flank of the volcano (see Gresta *et al.*, 1987).

The third swarm considered (7-10 May 1986) occurred (see table II) during a rest period of the volcano, with deep (10-26 km) earthquakes located on the eastern flank of the volcano. No intrusive episodes have been invoked by the literature for such time interval.

4. The analysis

For each earthquake considered, the FPFIT program gives a stereo projection of all orientations for *P*- and *T*-axes compatible with the available data. These features of the code were helpful to evaluate the quality of solutions avoiding those not enough constrained to be used in the stress inversion runs. Each FPS has assigned a weight (1 or 2) based on the solution quality, evaluated from the polarity distribution, from the existence of multiple solutions and from the number of discrepancies. By inverting FPS for stress directions, we avoided the limitations which are related to previous stress investigations based only on plotting of *P*- and *T*-axes.

With several faults we can search for a stress model that is compatible with all the slip directions, or which minimizes the differences between observations and predictions. A minimum of four different orientations of fault planes is needed for a unique estimate of *R* and of the three principal stress directions.

We calculated the stress tensor by inversion of FPS of earthquakes which occurred during the three above quoted sequences. FPS used for the inversion were considered after a critical evaluation of their quality. The retained ones are shown in fig. 2, while the related parameters are reported in table III. Strike-slip mechanisms seem to be prevalent, even if both direct and reverse dip-slip ruptures are also observed.

Since the principal fault planes were not known, both nodal planes of each mechanism

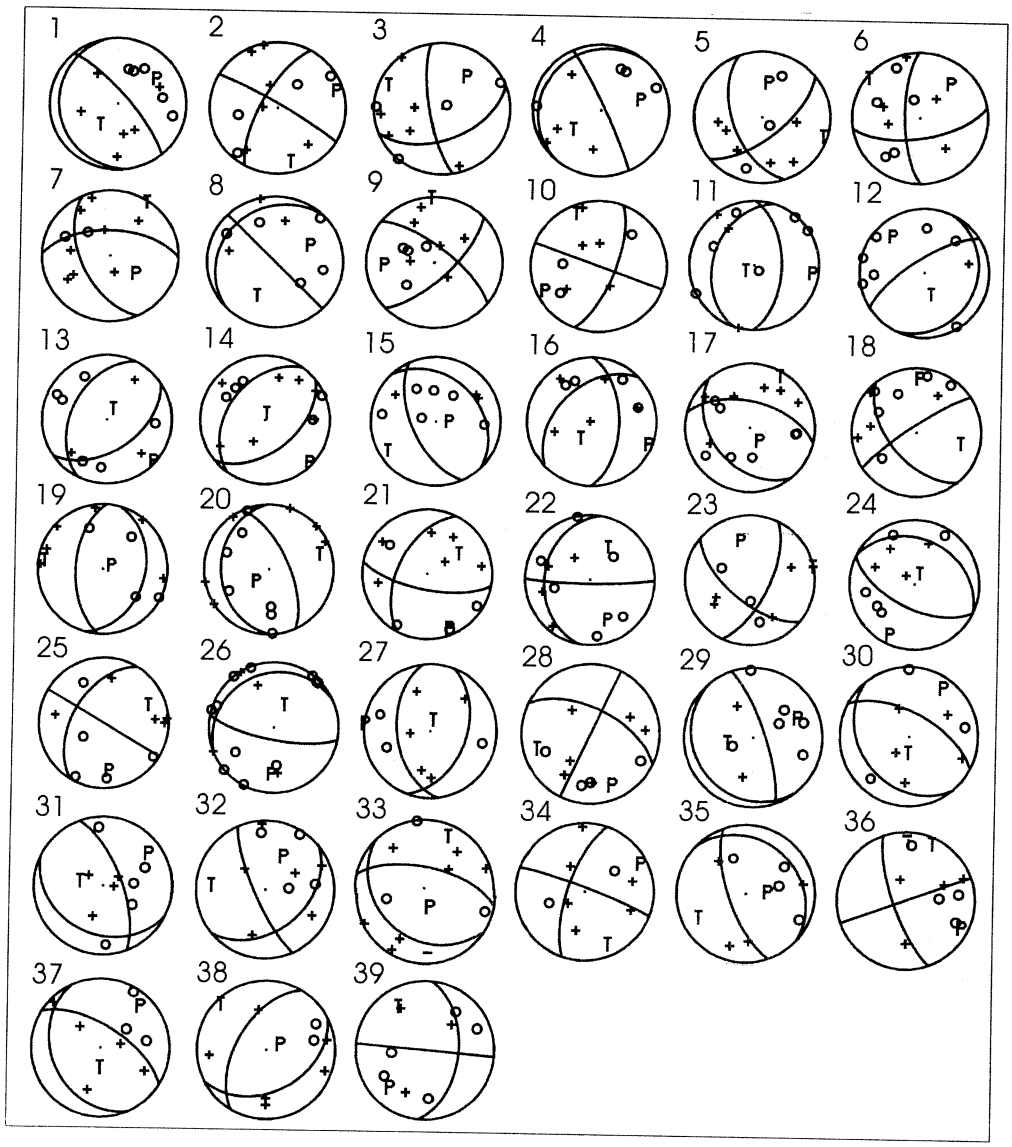

Fig. 2. Focal plane solutions relating the three considered seismic sequences. Numbering corresponds to that of table III.

have been tested independently against each stress model; the smallest of the two values was adopted as the misfit for that event. This choice minimized the difference between the observation and prediction in each case.

Results are shown in fig. 3a-c, and summarized in table IV. A first observation concerns the comparison of results obtained using both the «approximate» and the «exact» methods on the same data sets (see table IV). Only the mis-

Table III. Order number, date, origin time, magnitude, hypocentral parameters and FPSs of earthquakes selected for stress inversion among the three seismic swarms. *W* is the weight assigned to the FPS, while its sign indicates direct (+) or reverse (–) mechanism.

No.	Date	Origin time	*M*	Lat.	Long.	Depth (km)	Strike1 (°)	Dip1 (°)	Strike2 (°)	Dip2 (°)	W
1	830603	11:07	3.1	37-40.17	14-59.94	10.7	170	15	319	77	−1
2	830603	11:11	3.3	37-44.24	14-57.90	13.4	300	85	208	70	−2
3	830603	11:23	2.8	37-41.45	14-55.41	12.3	170	75	67	51	2
4	830603	14:19	2.6	37-42.63	14-59.26	10.6	335	85	218	11	−1
5	830604	01:19	2.6	37-40.49	14-59.91	11.3	50	65	159	54	2
6	830604	14:37	2.6	37-44.28	14-57.97	16.2	80	65	178	71	1
7	830604	18:35	3.0	37-46.40	14-53.26	19.4	155	55	270	58	1
8	830604	20:07	2.6	37-46.89	14-56.31	13.2	315	90	225	20	−1
9	830604	21:50	2.8	37-45.67	14-56.50	25.7	45	70	307	71	2
10	830604	23:35	2.5	37-45.70	14-54.88	19.3	290	90	20	70	2
11	841020	15:32	2.5	37-45.12	15- 4.90	4.2	360	55	197	36	−2
12	841020	16:17	2.6	37-44.03	15- 6.53	4.4	25	20	236	72	−1
13	841020	18:20	2.3	37-46.46	15- 1.78	1.6	55	50	205	43	−2
14	841022	15:18	2.8	37-44.24	15- 3.96	4.9	50	50	214	41	−1
15	841023	00:14	3.0	37-41.70	15- 8.12	1.7	155	60	315	31	1
16	841023	04:00	2.5	37-45.35	15- 4.59	5.6	360	55	225	44	−2
17	841023	14:35	2.5	37-43.87	15- 3.56	3.6	140	40	282	56	1
18	841024	02:27	2.4	37-45.57	15- 1.98	2.9	140	55	235	81	−1
19	841024	02:45	2.2	37-46.57	15- .16	2.6	15	35	182	55	1
20	841024	15:04	3.3	37-45.96	15- 4.38	4.2	335	65	177	26	1
21	841024	17:56	2.7	37-45.12	15- 1.49	7.7	100	70	206	52	−1
22	841026	02:24	2.5	37-44.10	15- 8.63	9.0	90	85	188	30	−2
23	841026	11:37	2.6	37-45.41	15- 5.20	0.1	25	65	128	63	1
24	841026	13:54	2.5	37-45.62	15- 4.32	3.2	115	60	295	30	−2
25	841026	16:04	2.7	37-41.69	15- 4.98	4.6	300	90	210	50	2
26	841028	15:17	3.0	37-47.29	15- 3.68	4.2	100	75	245	17	−2
27	860507	22:36	3.0	37-47.40	15- 6.08	11.7	20	45	172	48	−2
28	860508	00:50	3.0	37-44.16	15- 5.55	11.6	25	90	295	60	−1
29	860508	03:11	2.8	37-46.35	15- 5.12	15.8	140	15	340	75	−2
30	860508	06:27	2.8	37-45.33	15- 6.63	15.1	140	30	297	61	−2
31	860508	07:02	3.0	37-44.07	15- 3.66	26.0	115	30	339	67	−1
32	860508	13:22	3.4	37-44.41	15- 4.47	15.8	50	40	155	77	2
33	860509	01:41	3.2	37-46.38	15- 3.41	12.3	135	30	281	64	2
34	860509	02:21	2.6	37-45.64	15- 5.32	17.3	290	85	198	70	−1
35	860509	12:36	2.7	37-45.06	15- 4.49	10.8	160	70	312	22	1
36	860509	12:40	3.2	37-44.63	15- 7.29	16.8	160	75	70	90	−1
37	860509	14:37	2.8	37-44.83	15- 4.09	16.9	155	30	301	64	−2
38	860510	05:23	2.9	37-45.44	15- 7.38	10.3	210	55	62	39	1
39	860510	16:55	3.0	37-47.24	15- 4.02	10.7	5	50	275	90	2

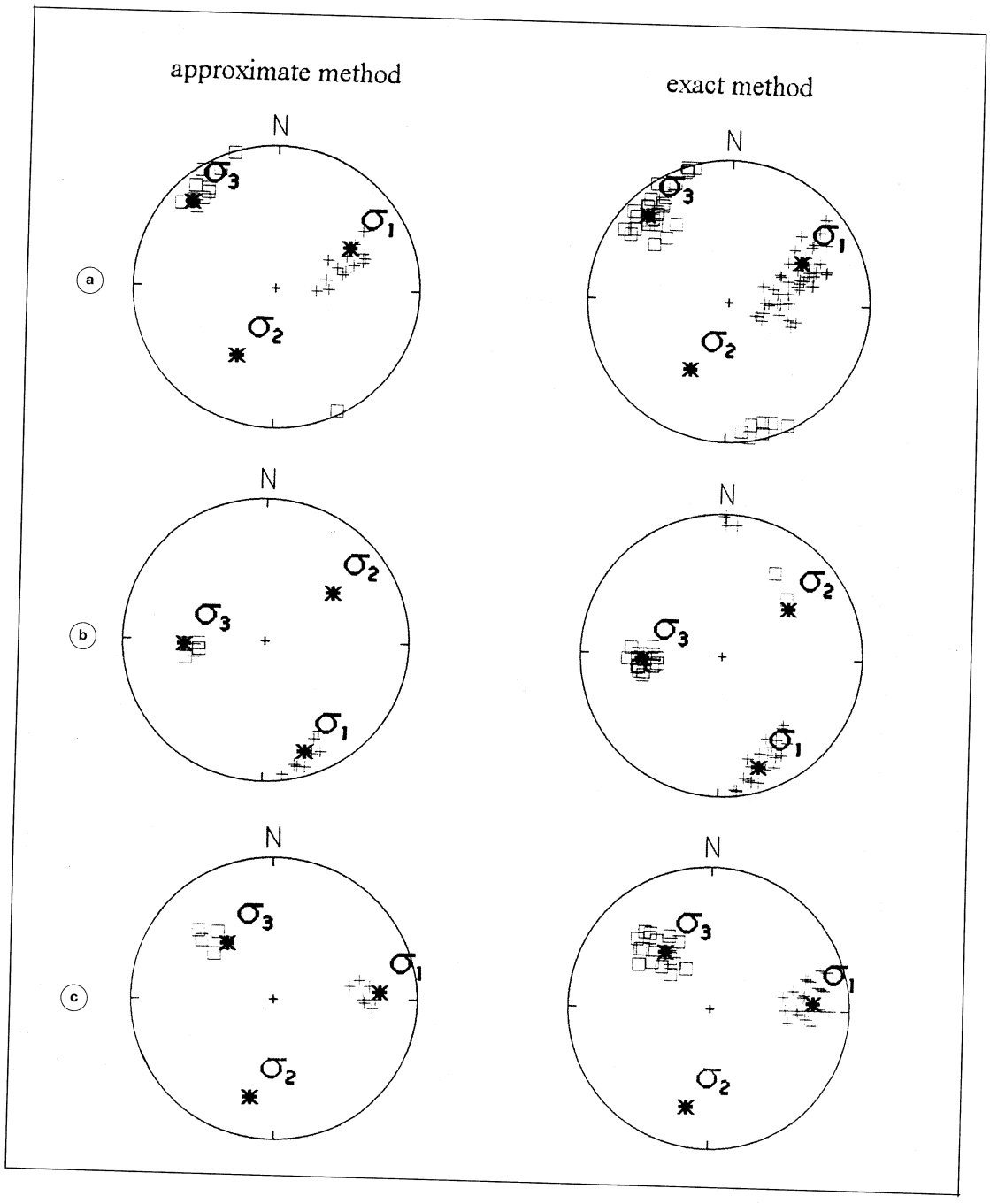

Fig. 3a-c. Results of the stress inversion for the three seismic sequences of: a) June 1983; b) October 1984; and c) May 1986 by use of the «approximate» and «exact» method. Asterisks indicate the σ_1, σ_2 and σ_3 orientations. Crosses and squares indicate the 90% confidence limits of σ_1 and σ_3 orientations, respectively.

Table IV. Results of the stress inversion for the three seismic sequences by use of both «approximate» and «exact» methods. *N*, *F* and *R*, are, respectively, the number of events in each data set, the average misfit (in degrees) and the relative magnitude of the principal stresses corresponding to the obtained stress solution.

Method	Seismic sequence	*N*	*F*	*R*	σ_1		σ_2		σ_3	
					Dip	Strike	Dip	Strike	Dip	Strike
Approximate	June, 1983	10	2.3	0.3	41	60	44	208	17	315
Approximate	October, 1984	16	4.5	0.1	18	160	42	53	43	267
Approximate	May, 1986	13	4.4	0.5	27	86	29	193	48	321
Exact	June, 1983	10	2.2	0.3	41	60	44	208	17	315
Exact	October, 1984	16	4.0	0.1	18	160	42	53	43	267
Exact	May, 1986	13	3.9	0.4	27	86	29	193	48	321

fit values (*F*) were slightly reduced by the use of the «exact» method, whereas both *R* and stress parameters were not significantly modified (table IV).

Generally speaking the *F*-values are acceptable for all three sequences, and the 90% confidence areas of the solutions (see fig. 3a-c) are small enough to draw the conclusion that stress is homogeneous in the crustal sub-volumes considered, in spite of the small number of events (see table IV).

The results of our analysis show that for the swarm of June 1983, (western side of the volcano, depth range 10-25 km), the principal stress axis σ_1 was about 40° dipping and N60°E striking. Conversely, the seismic sequence of October 1984 evidenced, in the shallow crust of the eastern flank, a σ_1 nearly horizontal and oriented about N-S. Finally, the swarm of May 1986 (eastern side, depth range 10-26 km) showed again a homogeneous stress with σ_1 27° dipping and around E-W striking.

5. Discussion and conclusions

More than 2400 earthquakes which occurred at Mt. Etna volcano during the time interval 1983-1986 have been relocated, and only those with better quality locations have been retained to compute focal mechanisms. The data set was strongly reduced to about 370 events, which allowed to *ca.* 100 reliable FPS.

In order to define the stress tensor acting on the area, we used the Gephart and Forsyth (1984) algorithm, with both «approximate» and «exact» methods, which minimizes the limits typical of all seismological approaches to the stress analysis. A question may arise on the significativity of results taken from few selected FPSs with respect to the whole seismicity affecting a given area; however, such a general question cannot be easily answered.

In detail, we have focused our attention on FPS relating to three seismic sequences, and the obtained stress directions are well defined in spite of the few events used. The results suggest space and/or time variation of the stress in the crust beneath the volcano body. In details: i) for the swarm of June 1983, which occurred on the western side of the volcano at depths ranging from 10 to 25 km during a flank eruption, stress is characterized by a σ_1 about 40° dipping, and N60°E striking; ii) the shallow seismic sequence of October 1984, started on the eastern flank just at the end of a long low rate eruption, points out a σ_1 nearly horizontal and oriented about N-S; iii) the swarm of May 1986, again on the eastern side, but at depths ranging 10-26 km, evidences again a homogeneous stress, but with a σ_1 27° dipping and *ca.* E-W striking.

These results disagree with the ones recently obtained by Cocina *et al.* (1997) by studying earthquakes which occurred during August 1990-September 1991. These authors

have found: i) homogeneous stress between 10 and 30 km of depth beneath Western Etna, with a low-dip, N-S trending σ_1 which agrees with the compressive tectonics of Sicily; ii) some stress heterogeneity at shallower depths in the same side of the volcano, whereas the stress inversion evidences a E-W orientation of σ_1 over the pre-eruptive period January 26-December 13, 1991; iii) the stress style changes across the 15°E meridian, and becomes more complex beneath Eastern Etna, where no uniform stress models are able to explain the available FPSs. They concluded that Western Etna is well included in the compressive domain of Western-Central Sicily, while Eastern Etna may represents a transition zone to the tensional domain of the Calabrian arc. The apparent contrasts between our results and the above quoted ones might depend on the short time periods that we have investigated, linked to well defined seismic sequences. In fact, our results support the hypothesis of time variations in the local stress field at Mt. Etna volcano, probably produced by magma intrusions. These ones should have occurred both in June 1983 and May 1986, when in the deeper crust (on the western side in the former case, and on the eastern one in the latter) two stress fields strongly in disagreement with the N-S compressive regional one have been found.

Bonaccorso *et al.* (1996) suggested a local inversion of the stress field acting in the upper crust ($h < 10$ km) of the volcano, which started less than two months before the onset of the 1991-1993 eruption, and has disappeared at its end.

We suggest that two episodes of magma intrusion have occurred at Etna on June 1983 and May 1986; they produced modifications in the local stress fields, and combined with the regional tectonics, determined the re-arrangement of the resulting stress tensor.

Conversely, the regional N-S compressional stress field was strongly acting at shallow depths on the whole eastern side of the volcano in October 1984; it should have contributed, as suggested by Patanè G. *et al.* (1994), to the end of a long subterminal eruption.

The present results support the hypothesis that the whole Etnean seismicity is strictly related to a complex stress field, fluctuating in time, space and intensity, due to the combined effects of both the compressive regional tectonics and the more or less frequent episodes of magma uprising into the crust.

Acknowledgements

The authors wish to thank G. Neri and E. Privitera for the use of some computer facilities. This work has been supported by MURST-40% grants.

REFERENCES

ANGELIER, J. (1979): Determination of the mean principal directions of stresses for a given fault population, *Tectonophysics*, **56**, 617-626.

ANGELIER, J. (1984): Tectonic analysis of fault slip data sets, *J. Geophys. Res.*, **89**, 5835-5848.

BEN-AVRAHAM, Z., M. BOCCALETTI, G. CELLO, M. GRASSO, F. LENTINI and L. TORTORICI (1990): Principali domini strutturali originatisi dalla collisione neogenico-quaternaria nel Mediterraneo Centrale, *Mem. Soc. Geol. It.*, **45**, 315-327.

BONACCORSO, A., F. FERRUCCI, D. PATANÈ and L. VILLARI (1996). Fast deformation processes and eruptive activity at Mount Etna (Italy), *J. Geophys. Res.*, **101**, 17467-17480.

BOUSQUET, J.C., S. GRESTA, G. LANZAFAME and C. PAQUIN (1987): Il campo degli sforzi attuali e quaternari nella regione dell'Etna: un esempio di evoluzione geodinamica in un contesto post-collisionale, *Mem. Soc. Geol. It.*, **38**, 483-506.

COCINA, O., G. NERI, E. PRIVITERA and S. SPAMPINATO (1997): Stress tensor computations in the Mount Etna area (Southern Italy) and tectonic implications, *J. Geodynamics*, **23**, 109-127.

CRISTOFOLINI, R., S. GRESTA, S. IMPOSA and G. PATANÈ (1988): Feeding mechanism of eruptive activity at Mt. Etna based on seismological and petrological data, in *Modeling of Volcanic Processes*, edited by C.Y. KING and R. SCARPA, *Earth Evol. Sci.* (Springer Verlag, Berlin), 73-93.

GASPERINI, P., S. GRESTA, F. MULARGIA and G. DISTEFANO (1992): Time and space clustering of Etna volcano earthquakes during the period May 1983-February 1987, *J. Volcanol. Geotherm. Res.*, **53**, 297-307.

GEPHART, J.W. (1990): Stress and the direction of slip on fault planes, *Tectonics*, **9**, 845-858.

GEPHART, J.W. and D.W. FORSYTH (1984): An improved method for determining the regional stress tensor using earthquake focal mechanism data: application to the San Fernando earthquake sequence, *J. Geophys. Res.*, **89**, 9305-9320.

GHISETTI, F. (1984): Recent deformation and the seismo-

genic source in the Messina Strait (Southern Italy), *Tectonophysics*, **109**, 191-208.

GLOT, J.P., S. GRESTA, G. PATANÈ and G. POUPINET (1984): Earthquake activity during the 1983 Etna eruption, *Bull. Volcanol.*, **47**, 953-963.

GRESTA, S. and G. PATANÈ (1983a): Variation of *b* values before the Etnean eruption of March 1981, *Pure Appl. Geophys.*, **121**, 287-295.

GRESTA, S. and G. PATANÈ (1983b): Changes in *b* values before the Etnean eruption of March-August 1983, *Pure Appl. Geophys.*, **121**, 903-912.

GRESTA, S. and G. PATANÈ (1987): Review of seismological studies at Mount Etna, *Pure Appl. Geophys.*, **125**, 951-970.

GRESTA, S., J.P. GLOT and G. PATANÈ (1985): Studio di meccanismi focali di terremoti etnei, in *Proceedings of the 4th Annual Meeting GNGTS*, **2**, 809-815.

GRESTA, S., J.P. GLOT, G. PATANÈ, G. POUPINET and S. MENZA (1987): The October 1984 seismic crisis at Mt. Etna. Part 1: space-time evolution of the events, *Ann. Geophysicae*, **5B**, 671-680.

GRESTA, S., V. LONGO and A. VIAVATTENE (1990): Geodynamic behaviour of eastern and western sides of Mt. Etna, *Tectonophysics*, **179**, 81-92.

HIRN, A., A. NERCESSIAN, M. SAPIN, F. FERRUCCI and G. WITTLINGER (1991): Seismic heterogeneity of Mt. Etna: structure and activity, *Geophys. J. Int.*, **105**, 139-153.

LEE, W.H.K. and J.C. LAHR (1975): HYPO 71: a computer program for determining hypocenter, magnitude and first motion pattern of local earthquakes, *USGS Open-File Report 75/311*, pp. 116.

MICHAEL, A. (1984): Determination of stress from slip data: Faults and folds, *J. Geophys. Res.*, **89**, 11517-11526.

MICHAEL, A. (1987): Use of focal mechanisms to determine stress: a control study, *J. Geophys. Res.*, **92**, 357-368.

PARKER, R.L. and M.K. MCNUTT (1980): Statistics for the one-norm misfit measure, *J. Geophys. Res.*, **85**, 4429-4430.

PATANÈ, D., T. CALTABIANO, E. DEL PEZZO and S. GRESTA (1992): Time variation of *b* and Q_c coefficients at Etna volcano (1981-1987), *Phys. Earth Planet. Inter.*, **71**, 137-140.

PATANÈ, D., F. FERRUCCI and S. GRESTA (1994): Spectral features of microearthquakes in volcanic areas: attenuation in the crust and amplitude response of the site at Mt. Etna, Italy, *Bull. Seism. Soc. Am.*, **84**, 1842-1860.

PATANÈ, G., A. MONTALTO, S. IMPOSA and S. MENZA (1994): The role of regional tectonics, magma pressure and gravitational spreading in earthquakes of the eastern sector of Mt. Etna volcano, *J. Volcanol. Geotherm. Res.*, **61**, 253-266.

REASENBERG, P.A. and D. OPPENHEIMER (1985): Fortran computer programs for calculating and displaying earthquake fault-plane solutions, *USGS Open-File Report 85/379*, pp. 109.

RIVERA, L. and A. CISTERNAS (1990): Stress tensor and fault plane solutions for a population of earthquakes, *Bull. Seism. Soc. Am.*, **80**, 600-614.

SCARPA, R., G. PATANÈ and G. LOMBARDO (1983): Space-time evolution of seismic activity at Mount Etna during 1974-1982, *Ann. Geophysicae*, **1**, 451-462.